Pergamon

Int. J. Heat Mass Transfer. Vol. 38, No. 6, pp. 969–977, 1995

0017-9310/95 $9.50+0.00

0017-9310(94)00224-X

Pool boiling heat transfer—I. Measurement and semi-empirical relations of detachment frequencies of coalesced bubbles

T. KUMADA and H. SAKASHITA

Department of Nuclear Engineering, Faculty of Engineering, Hokkaido University, North 13, West 8, Kita-ku, Sapporo 060, Japan

and

H. YAMAGISHI

Department of Mechanical Engineering, Kushiro National College of Technology, West 2-32-1, Otanoshike, Kushiro 084, Japan

(*Received* 15 *July* 1993 *and in final form* 20 *July* 1994)

Abstract—Measurements were made of the detachment frequency of coalesced bubbles from circular, horizontal 2–30 mm diameter disks and thin, horizontal 0.2–3 mm diameter wires at high heat fluxes and atmospheric pressure. The disks are a heated copper cylinder and a sintered brass plate through which nitrogen gas is blown. Detachment frequencies from disks and thin wires were measured with water, ethanol and Freon-113. The bubble frequency was determined with high speed video. Semi-empirical correlations of bubble frequencies are proposed for both disks and thin wires. The correlations were derived by the dimensional analysis of force balance equations relevant to the behavior of bubbles.

1. INTRODUCTION

Based on a series of studies, Katto and Yokoya [1, 2] have presented the formulation of a model for saturated pool boiling CHF. The model is expressed by the following energy balance relationship:

$$\tau_d q_{CHF} = \delta_l \rho_l H_{fg} \tag{1}$$

where δ_l is the thickness of the macrolayer at formation, and τ_d is the hovering period of the vapor mass. It is therefore necessary to determine the correlation of δ_l and τ_d, to obtain the CHF correlation based on relation (1). To determine CHF correlations, δ_l and τ_d must be determined in a manner which avoids physically unsustainable assumptions and approximations.

For the isolated bubble region, bubble frequencies f and diameters D_b at detachment are of major importance to understand nucleate boiling heat transfer, and there are numerous experimental and theoretical studies of this. The relations between f and D_b for an isolated bubble region in nucleate boiling are reported by Jakob and Linke [3], Fritz and Ende [4], Peebles and Garber [5], Zuber [6], Yamagata *et al.* [7] and others. They suggested correlations similar to

fD_b = constant or proportional to

$$\{g(\rho_l-\rho_v)/\rho_l\}^{1/4}. \tag{2}$$

Frederking and Daniels [8] have developed a theoretical correlation of f and D_b during film boiling as

$$fD_b^{1/2} \propto \{g(\rho_l-\rho_v)/\rho_l\}^{1/2}. \tag{3}$$

Ivey [9] suggested the following three regions where the experimental data of f correlated differently:

(a) hydrodynamic region:

$$fD_b^{1/2} = 0.9g^{1/2} \tag{4}$$

(b) transition region:

$$fD_b^{3/4} = 0.14g^{1/2} \tag{5}$$

(c) thermodynamic region:

$$fD_b^2 = \text{constant}. \tag{6}$$

The 0.14 in equation (5) is different from the original 0.44, due to the differences in units, and correlation (4) may be for coalesced bubbles and equation (6) for isolated bubbles. Ivey provided a theoretical explanation for the variation of measured bubble frequencies and diameters in the hydrodynamic and thermodynamic regions.

Cole [10] measured the frequency for the coalesced bubble region in water near CHF with a 5 mm wide, 0.15 mm thick horizontal ribbon and proposed the correlation

$$fD_b^{1/2} = \{(4/3)g(\rho_l-\rho_v)/\rho_l\}^{1/2}. \tag{7}$$

Correlation (7) is derived by assuming a balance between buoyancy and drag (drag coefficient constant).

NOMENCLATURE

a, b	short and long axes of oblate rotary ellipse [m]
C	constant in the correlation
C_D	drag coefficient
C_0	constant in the drag coefficient
D	diameter of disk [m]
D_b	bubble diameter at departure [m]
d	diameter of wire or tube [m]
f	frequency of bubble detachment [s^{-1}]
G_0	blowing velocity of gas or vapor, $q/\rho_v H_{fg}$ [m s^{-1}]
$G_0 S$	blowing rate of gas or vapor [m^3 s^{-1}]
g	gravitational acceleration [m $s^{2^{-1}}$]
H_{fg}	latent heat of evaporation [J kg^{-1}]
q, q_{CHF}	heat flux, critical heat flux [W m^{-2}]
r, R	radius of growing and detached bubbles [m]
s	distance between center of bubble and heated surface [m]
S	area of sintered brass or heater disk [m^2]
t	time [s]
V, V_d	volume of growing and detached bubbles [m^3]
u_b	rising velocity of bubbles [m s^{-1}].

Greek symbols

δ_l	mean thickness of macrolayer [m]
μ_l	viscosity of liquid [Pa s]
ν_l	dynamic viscosity of liquid [m^2 s^{-1}]
ξ	11/16, fraction of liquid accompanying a growing bubble
ρ_l, ρ_v	density of liquid and vapor [kg m^{-3}]
σ	surface tension [N m^{-1}]
τ_d	hovering period of coalesced bubbles [s].

Dimensionless quantities

M	$g(\rho_l-\rho_v)\nu_l^4\rho_l^2/\sigma^3$, Molton number
Re_d	$2Ru_b/\nu_l$, bubble Reynolds number
$\bar{R}$	r/R
$\bar{S}$	s/R
$\bar{T}$	t/τ_d.

It must be noted that the kinetic viscosity of liquid, surface tension, and geometric parameters and orientation of the heating elements are not considered in correlations (2)–(7). Bubble dynamics [11], however, teaches us that bubble motion strongly depends on the bubble Reynolds number, Molton number, and the geometry and orientation of heating elements. This makes it difficult to establish accurate values of detachment frequencies for specific heaters with the available correlations of detachment frequency. It is therefore necessary to derive accurate correlations for bubble frequencies for specific heaters of given geometries and orientations. Such correlations can be used to determine the macrolayer thickness with CHF data or to obtain CHF correlations with the macrolayer thicknesses, based on relation (1).

This series of papers relates to the formulation for various aspects of pool boiling phenomena, such as the detachment frequency of coalesced bubbles $f\,(=1/\tau_d)$, the thickness of a macrolayer δ_l, the CHF for horizontal and vertical thin wires. The major purpose of this first paper is to report the detachment frequency of vapor masses (coalesced bubbles) and to obtain semi-empirical correlations of detachment frequencies for horizontal disks and thin wires. With such correlations, the thickness of the macrolayer can be determined from the energy balance relation (1), and this will be reported in the second paper of this series.

2. EXPERIMENTAL APPARATUS AND METHODS OF MEASUREMENT

2.1. *Horizontal disks*

Circular disks have often been used to study boiling heat transfer. In the present experiment, bubble frequencies were measured with heating disks of copper for boiling and with disks of sintered brass through which nitrogen gas was blown. Figure 1 shows the equipment and the sintered brass disk (50 mesh par-

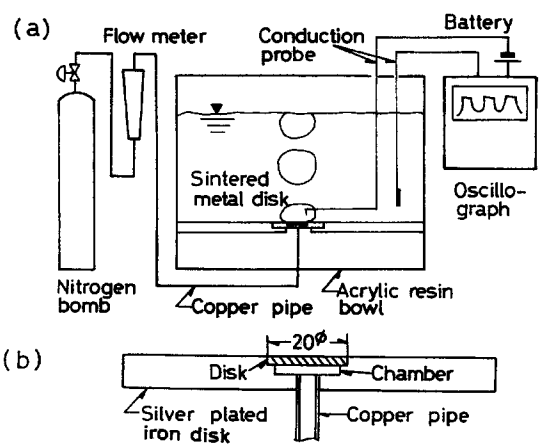

Fig. 1. Experimental apparatus for gas blowing. (a) Diagram of the experimental apparatus. (b) Details of blowing surface made of sintered metal.

ticle radius). The pipe from the gas bomb to the disk is a 4 mm inner diameter copper tube. Katto and Yokoya [2] measured the volumetric growth rate of coalesced bubbles growing on a circular 10 mm diameter horizontal disk near CHF and concluded that the rate of increase in volume is nearly constant throughout the process of bubble growth. To achieve a constant blowing rate of nitrogen gas through the sintered brass disk, the pressure loss in the pipe was made so large that the pressure loss through the sintered brass disk may be neglected. The horizontal plate surrounding the disk and the vessel are large compared with the diameter of the disk and the depth of liquid in the vessel is more than 200 mm to avoid effects of liquid level and size of vessel. The bubble frequency was measured with 2–30 mm diameter disks in water, Freon-113 and ethanol. The movement of bubbles was recorded with a high speed video camera (max. 2066 f s^{-1}) and images on a television screen were used to count bubble frequencies.

Boiling experiments were also performed with 5–30 mm diameter heated copper disks. The heat flux was determined by measuring temperatures with three thermocouples embedded at the center of the copper cylinder. The boiling surfaces were polished to emery number 60. Measurements were performed after the thermal equilibrium of the equipment had been fully established. The blowing rate of vapor, G_0S, from the surfaces was calculated based on the heat flux.

Katto and Yokoya [2] measured the detachment frequency of coalesced bubbles from a 10 mm diameter horizontal disk and pointed to three modes of bubble detachment:

(a) large spherical bubbles whose behavior is not affected by preceding bubbles;

(b) relatively small bubbles which detach from the heating surface just after the detachment of large bubbles;

(c) smaller bubbles detaching sequentially from the heating surface.

We observed a similar behavior of coalesced bubbles, and the appearance of different modes varies with the diameter of the boiling or blowing surfaces and the blowing rate of vapor or gas. The bubble frequency correlations obtained in this paper are used in the second paper of this series to determine the macrolayer thickness based on relation (1), using CHF data previously reported and measured with an upward facing 20 mm diameter disk heater. The CHF depends on the average number of macrolayers formed per unit time on heaters of high thermal conductivity and large heat capacity, and the mean bubble frequency over a few seconds. The effect of small variations in bubble frequency pointed out by Katto and Yokoya [2] may play an important role for heaters of small effective thermal conductivity and heat capacity such as thin wire or foil.

2.2. *Horizontal wires*

Figure 2 shows the boiling apparatus in the thin wire experiments. The nichrome wires were 0.1, 0.2, 0.3 and 0.5 mm diameter and the lengths were from 80 to 180 mm. The stainless steel wires were 1.0, 1.2 and 1.5 mm diameter, the tubes 2 and 3 mm in diameter, and all 180 mm long. The boiling situation was recorded by a high speed video camera at the central part of the wires and the bubble frequency was determined with images on a television screen. Power was supplied to the wires by direct or alternating currents. The alternating current was for wires above 0.8 mm diameter. Heat flux was determined by measuring the voltage drop between the terminals of the heating wire and the total passed current.

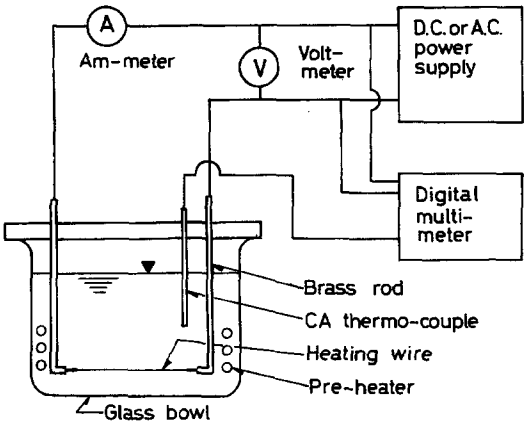

Fig. 2. Experimental apparatus for boiling on thin wires.

To calculate bubble volumes it was assumed that bubbles were ellipsoidal with semiaxes of b, c ($b = c$) and the main axis of a parallel to the direction of gravity for wires thinner than 0.5 mm in water and thinner than 0.3 mm in other liquids. The bubble volume is given by $V = (\pi/6)ab^2$ and the bubble radius by

$$R = (1/2)(ab^2)^{1/3}. \tag{8}$$

The shape of bubbles produced around wires thicker than 0.8 mm in water and 0.5 mm in other liquids is very different from spherical. The average volume of each coalesced bubble in this case, is determined from the total volume of vapor generated per second divided by a multiplier for the detachment frequency and the number of areas generating coalesced bubbles. The radius of the coalesced bubbles is determined from the average volume of the bubbles assuming them to be spherical. The minimum volume of bubbles is obtained from the rate of generated vapor divided by a multiplier for the maximum number of bubble generating locations and the detachment frequencies (the maximum volume is obtained with their minima values). The deviation between minimum and maximum bubble volumes and detachment frequencies are 30 and 20%, respectively. The detachment frequencies in Figs. 4 and 5 are the arithmetic mean values of the minima and maxima, and each frequency in Figs. 4 and 5 fluctuated within a band of about 10%.

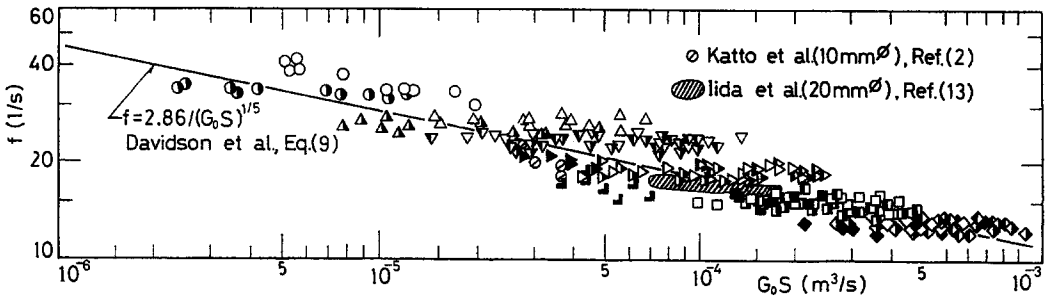

Fig. 3. Detachment frequency of upward disks.

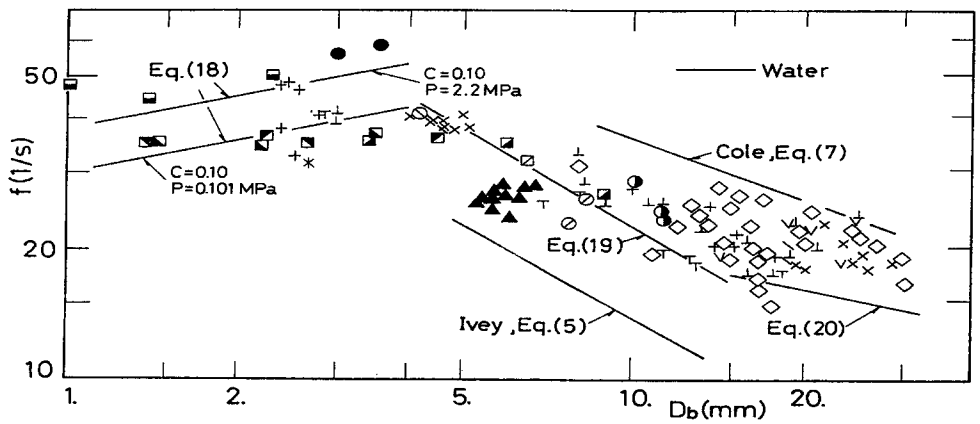

Fig. 4. Reported detachment frequencies of coalesced bubbles.

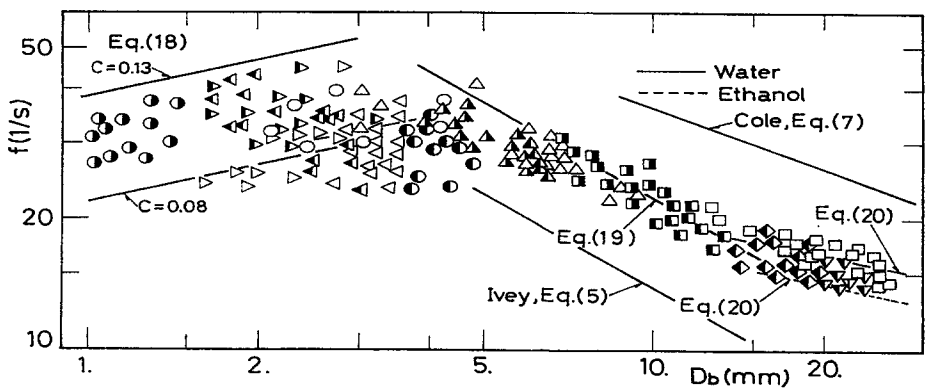

Fig. 5. Measured detachment frequency for thin wires.

3. EXPERIMENTAL RESULTS

3.1. *Horizontal disks*

Figure 3 shows detachment frequencies of coalesced bubbles vs the blowing rate G_0S. Table 1 shows the symbols used in Fig. 3. In the range of blowing rates $G_0S > 10^{-5}$ m^3 s^{-1}, bubble frequencies vary with the diameter of the disks, but are almost independent of the vapor or gas blowing rate. This was also found by Iida and Kobayasi [12], Katto and Yokoya [2], and Honda and Nishikawa [13]. In the range $G_0S < 1 \times 10^{-5}$ m^3 s^{-1}, bubbles blown from disks smaller than 3.5 mm diameter remain for longer times at region III of the drag coefficient in Fig. 7, due to the slow growth rate in volume. The bubble frequency decreases with increasing blowing rate, because drag coefficient increases sharply in this region, as shown in Fig. 7. The solid line in Fig. 3 shows the following analytical correlation, derived from the force balance between buoyancy and inertia of the liquid

Table 1. Detachment frequency for upward facing disks

Diameter of disk [mm]	Water	Ethanol	R-113
2	○	◐	—
3.5	△	◭	—
5	▽	▼	▼
10	▷▶	▶	▶
16	▟	—	—
20	□■	◧	◨
30	◇◆	◆	◆

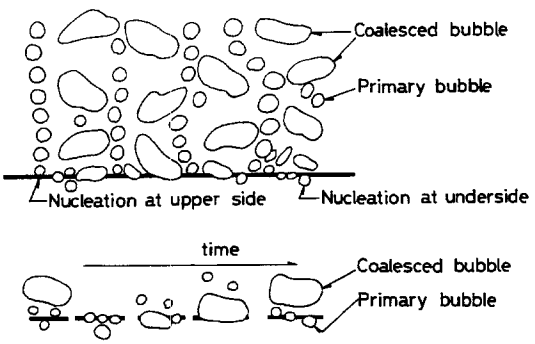

Fig. 6. Bubble behavior on very thin wires in water.

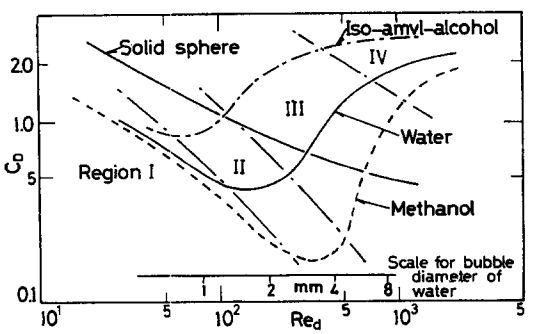

Fig. 7. Drag coefficients and bubble Reynolds numbers.

accompanying the growing bubbles, by Davidson *et al.* [14],

$$f = 2.86/(G_0 S)^{1/5} \tag{9}$$

where S is the cross-section of a blowing tube. Correlation (9) fairly accurately predicts the gross variation in the data against the blowing rate $G_0 S$, but depends on $G_0^{1/5}$ of the blowing velocity when S is constant, while the data are independent of G_0 when S is constant.

3.2. *Horizontal thin wires*

Data on bubble frequencies vs bubble diameter reported by various authors and those obtained here are summarized in Figs. 4 and 5. Tables 2 and 3 show details of the measurement and the symbols used in Figs. 4 and 5. The data obtained with $d < 0.5$ mm wires for water and $d < 0.3$ mm for other liquids are widely scattered. With these wires the diameter of bubbles is smaller and the detachment frequency higher when bubbles generate on the upper side of wires than when they nucleate on the underside. Bubbles which nucleate on the undersides of wires sometimes move downward for one or two diameters before they slowly rise. This provides an opportunity for absorbing surrounding small bubbles to become larger.

For single bubbles in stagnant liquids, the drag coefficient of bubbles is often expressed with the parameter $Re_d M^{0.25}$ [5]. It is, however, very difficult in the present experiment to measure and define the relative velocity between bubbles and their surrounding liquid due to the complicated behavior of bubbles and liquid flow and bubble coalescence. The detachment frequency is therefore not plotted against the parameter including $Re_d M^{0.25}$, but is plotted against the diameter of bubbles. In Figs. 4 and 5 the detachment frequency is fairly scattered, but the data show different variations dependent on the diameter of bubbles, and the detachment frequency is approximately classified into three bubble diameter regions (I–III).

(a) *Region* I ($D_b \lesssim 4$ mm). The detachment frequency of coalesced bubbles was measured by Bobrovich and Mamontova [15] with a horizontal ribbon heater (2 mm wide, 0.5 mm thick) in water at 0.1–5 MPa. Their measurements took place in the low heat flux region and the diameter of the bubbles was 1–3 mm. Most of the data by Bobrovich and Mamontova may represent coalesced bubbles, except the data on small diameters at lower pressures. The data by Bobrovich and Mamontova depend on pressure and very weakly on the diameter of bubbles.

In the present measurements, the detachment frequency of coalesced bubbles near CHF was obtained with water, ethanol and Freon-113. The detachment frequency of coalesced bubbles is very scattered, and also depends weakly on the bubble diameter. Most coalesced bubbles with thin wires, 0.1 and 0.3 mm, were formed by the coalescence of several primary bubbles. A primary bubble produced at the underside of wires grows as an embryo and coalesces with the surrounding primary bubbles (refers to Fig. 6). The differences in detachment frequencies between the data here and the data of Bobrovich and Mamontova for coalesced bubbles depend on whether bubbles envelop the heating element or not. The bubbles measured by Bobrovich and Mamontova did not envelop the ribbon heater, because the heater was too wide, and the detachment frequency is close to the maximum in the present measurements. The data on coalesced bubbles in this region scatter greatly, and it is difficult to determine the dependence of detachment frequency on bubble diameter. The detachment frequency of coalesced bubbles in both measurements

Table 2. Detachment frequency for thin wires

Reference	Authors	Diameter of wire [mm]	Liquid	Pressure [MPa]	Symbol
[10]	Cole	5 × 0.15	Water	0.101	◇
[16]	Perkins and Westwater	9.5	Methanol	0.101	●
[13]	Honda and Nishikawa	0.5	Water	0.101	▲
[15]	Bobrovich and Mamontova	2 × 0.5	Water	0.098	◪
				0.49	◩
				1.08	◥
				2.06	◥
				5.2	■
[9]	Ivey	Unknown	Water	0.101	⊘ ⌀
[14]	Davidson and Schüler	Tube 2.3	Water	0.101	⊥ ⊤
		dia. 2.65			× +
		4.8			v

appears to be weakly dependent on the bubble's diameter, and we set it to be $f \propto R^{1/4}$.

For water and ethanol at atmospheric pressure and lower heat fluxes, the detachment frequency of primary bubbles for 0.1–0.3 mm diameter wires increases with $R^{1/2}$ with increasing heat flux and depends strongly on the circumferential position on the wires where nucleation occurs.

The dependence of detachment frequency on bubble diameter for thin horizontal wires is very different from that suggested by Jakob and Linke [3] for a vertical cylindrical surface, $fD_b = 280$ m h^{-1}; by Yamagata *et al.* [17], for a large horizontal plate; $fD_b = 350$ m s^{-1}; by Zuber [18], $fD_b = 330$ m h^{-1}. These differences may be due to the different orientation and geometries of the heating elements and the resulting different flow patterns of the liquid around them.

(b) *Region* II (4 mm $\leqslant D_b \leqslant$ 15 mm). Here the bubble detachment frequency is proportional to $R^{-3/4}$. The dependence of detachment frequency on bubble diameter is the same as in the transition region of Ivey [9]. The values calculated by correlation (5) of Ivey are shown in Figs. 4 and 5, and they are much smaller than other measured data.

(c) *Region* III ($D_b \gtrsim$ 15 mm). The detachment frequency by Cole [10] is somewhat larger than the present measurements because their ribbon heater was 5 mm wide and 0.15 mm thick, corresponding to a circular wire diameter of about 3.3 mm. These values, calculated with correlation (7) by Cole, are much larger than the present and Cole's data. Cole's data depend weakly on the diameter of the bubbles. It is difficult to determine the exact dependence of detachment frequency on bubble diameter based on Cole's data. The scattering of the data is considerable and the dependence on the bubble diameter is weaker than that suggested by Cole. On the basis of the data in both Figs. 4 and 5, the bubble detachment frequencies were determined to be proportional to $R^{-1/4}$.

Table 3. Detachment frequency for thin wires

Diameter of wire [mm]	Water	Ethanol	R-113
0.1	▷	▶	—
0.2	◁	◀	
0.3	○	◐	◑
0.5	△	▲	▲
1.2	□	◧	◨
2.0	—	◆	—
3.0	—	▼	—

4. DERIVATION OF THE SEMI-EMPIRICAL CORRELATIONS

4.1. *Drag coefficient and bubble diameter*

Figure 7 shows qualitative variations in the drag coefficient with bubble Reynolds number Re_d for single bubbles of constant volume rising in pure liquids, cited from ref. [11]. The drag coefficient curves in Fig. 7 are different for different liquids, mainly due to differences in the Molton number M. The bubble diameter at the terminal velocity in water at room temperature is shown in the lower part of Fig. 7. The bubble diameter in region I is smaller than 1 mm for water at atmospheric pressure and room temperature, and the drag coefficient varies with Stokes' law. The diameter of bubbles in region III is larger than 3 mm and the drag coefficient increases steeply with increasing bubble Reynolds number. The drag coefficient in region II has a minimum in the transition from region I to III. The drag coefficient in region IV is almost constant, independent of bubble Reynolds number and kind of liquid. Bubbles in this region rise vertically and are mushroom shaped.

The bubble frequencies in Figs. 4 and 5 are classified into three regions, I–III, depending on the bubble diameter. The behavior of bubbles in the three regions in Figs. 4 and 5 corresponds roughly to that of bubbles in regions II–IV in Fig. 7, which are not growing. The relative velocity of a growing bubble to its surrounding liquid is much smaller than that of bubbles

which are not growing, because the growing bubble is accompanied by much liquid. This is why the bubble diameter in regions I–III in Figs. 4 and 5 become much larger than the corresponding ones of regions II–IV in Fig. 7.

4.2. *Forces acting on bubbles*

The drag coefficients in Fig. 7 are obtained by the rising velocity of bubbles with constant volume. With boiling or gas blowing, however, bubbles increase in volume and change in shape with increasing volume, and the various forces acting on the bubbles change with changes in the volume and shape. There is large inertia due to the liquid mass accompanying a growing bubble, while little inertia acts on bubbles of constant volume. Liquid flow around bubbles or heating surfaces strongly depends on the geometry and orientation of the heating elements.

With upward facing circular surfaces the bubble diameter stays in region IV in Fig. 7 during most of the growth of bubbles. With thin wires bubble diameters are generally smaller than those with upward facing disks and the bubble Reynolds number ranges widely from region II to region IV in Fig. 7. Surface tension which causes bubbles to stick to a wire and reaction forces from the wire can be neglected, except for the smaller bubbles. It is generally very difficult to obtain analytical solutions to the force balance equation when considering all these forces. The authors here applied dimensional analysis to derive bubble frequency correlations, and the solution is in the form of a power function of the parameters, which is very convenient to use.

4.3. *General correlation of detachment frequency*

It is assumed that the shape of bubbles does not change. The force balance acting on a bubble is expressed by

$$Vg(\rho_l-\rho_v) = \mathrm{d}/\mathrm{d}t\{(\xi\rho_l+\rho_v)V(\mathrm{d}s/\mathrm{d}t)\} + (\pi/4)D^2\rho_l\{r\,\mathrm{d}^2r/\mathrm{d}t^2+3/2(\mathrm{d}r/\mathrm{d}t)^2\} + (C_0\rho_l/2)(Re_d M^{0.25})^m\pi r^2(\mathrm{d}s/\mathrm{d}t)^2+2\pi\beta\sigma(r-s). \quad (10)$$

The second term on the right-hand side is the reaction force from the heating surface, which can be neglected for thin wires. The third term is the drag, which is expressed with the general form $C_D = C_0(Re_d M^{0.25})^m$. Equation (10) does not accurately express the force balance acting on the bubble, because the effect of the liquid flow on the frequency around a bubble and the deformation of bubble shape is neglected. These effects may be included in a constant and exponents in the correlation, which are determined to fit with the data, as the effects may be at least partly due to the forces considered in relation (10). The r, s, and t terms are nondimensionalized in the form $r/R = \bar{R}$, $s/R = \bar{S}$ and $tf = \bar{T}$. Substituting $r = R\bar{R}$, $s = R\bar{S}$ and $t = \bar{T}/f$ into equation (10) gives the following correlation:

$$(4\pi/3)\bar{R}^3 = (4\pi/3)\underline{\{(\xi\rho_l+\rho_v)/g(\rho_l-\rho_v)\}Rf^2} \times \mathrm{d}/\mathrm{d}\bar{T}(\bar{R}^3\,\mathrm{d}\bar{S}/\mathrm{d}\bar{T}) + (\pi/4)\underline{\{\rho_l/g(\rho_l-\rho_v)\}(D^2f^2/R)} \times \{\bar{R}\,\mathrm{d}^2\bar{R}/\mathrm{d}\bar{T}^2+(3/2)(\mathrm{d}\bar{R}/\mathrm{d}\bar{T})^2\} + \pi(C_0/2) \times \underline{\{\rho_l/g(\rho_l-\rho_v)\}}(M^{0.25}/\nu_l)^m R^{2m+1}f^{m+2}(\mathrm{d}\bar{S}/\mathrm{d}\bar{T})^{m+2} + 2\pi\beta\underline{\{\sigma/g(\rho_l-\rho_v)R^2\}}(\bar{R}-\bar{S}). \quad (11)$$

The solution for R and f is assumed to be expressed with a power function of the underlined dimensionless coefficients in the first to fourth terms on the right-hand side of equation (11), as

$$[\{(\xi\rho_l+\rho_v)/g(\rho_l-\rho_v)\}Rf^2]^i[\{\rho_l/g(\rho_l-\rho_v)\}(D^2f^2/R)]^j \times [\{\rho_l/g(\rho_l-\rho_v)\}(M^{0.25}/\nu_l)^m R^{2m+1}f^{m+2}]^k \times [\sigma/\{g(\rho_l-\rho_v)R^2\}]^l = C \quad (12)$$

where the exponents i, j, k, l and m are unknown constants and determined with the experimental data of bubble frequencies. Correlation (12) is rearranged for $f \propto f(R)$ as

$$f = C\{g(\rho_l-\rho_v)/(\xi\rho_l+\rho_v)\}^{i/z}\{g(\rho_l-\rho_v)/\rho_l D^2\}^{j/z} \times [\{g(\rho_l-\rho_v)/\rho_l\}(\nu_l/M^{0.25})^m]^{k/z}\{g(\rho_l-\rho_v)/\sigma\}^{l/z}/R^{\{i-j+k(2m+1)-2l\}/z} \quad (13)$$

where $z = 2i+2j+k(m+2)$. Semi-empirical correlations of bubble frequencies are obtained by determining the exponents and the constant to fit correlation (13) with the measured data.

4.4. *Bubble frequency correlation*

(A) *Horizontal disks.* With the blowing rate $10^{-5} \leqslant G_0S \leqslant 10^{-3}$ m^3 s^{-1}, bubbles on disks larger than 5 mm in diameter mainly grow and detach in drag coefficient region IV after quickly passing through regions I–III in Fig. 7, because the bubble diameter quickly grows to diameters beyond 10 mm. Surface tension can be neglected, because the bubble growth rate and the bubble size are large and the inertia and buoyancy are much larger than the surface tension. Exponent l in correlation (13) can, then, be set to zero. The measured frequencies in Fig. 3 do not depend on the blowing rate G_0S and are proportional to $1/D^{1/3}$. The bubble frequency is assumed independent of the Molton number in the region. With $l = 0$ and $j/z = 1/6$ in equation (13), and $\xi\rho_l+\rho_v$ approximated by $\xi\rho_l$, the relation becomes

$$f = C\{g(\rho_l-\rho_v)/\rho_l\}^{5/9}/(\nu_l D^3)^{1/9}. \quad (14)$$

The constant is determined to achieve the best fit with the data,

$$f = 0.215\{g(\rho_l-\rho_v)/\rho_l\}^{5/9}/(\nu_l D^3)^{1/9}. \quad (15)$$

The calculated values by correlation (15) and the measured ones are shown in Fig. 8 against the blowing rate G_0S, and they agree quite well.

(B) *Horizontal thin wires.* Bubble detachment fre-

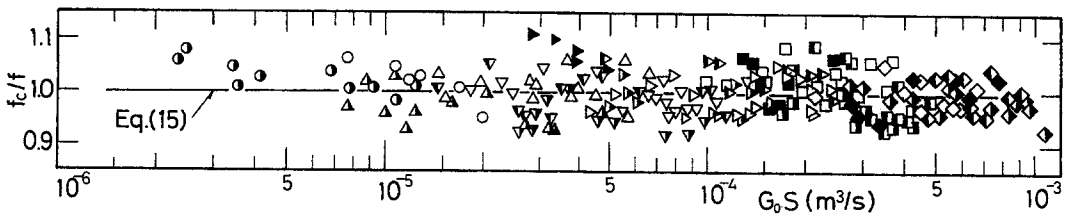

Fig. 8. Comparison of correlation (15) with data.

quencies with thin wires are generally larger than with horizontal disks, as shown in Figs. 4 and 5. This is because the induced flow of liquid around thin wires is faster than that around a horizontal disk. In thin wires the reaction force from the contact area between bubbles and the heating wires can be neglected, giving $j = 0$ in correlation (13). The resulting correlation is

$$f = C\{g(\rho_l-\rho_l)/(\xi\rho_l+\rho_v)\}^{i/Y} \times [\{g(\rho_l-\rho_v)/\rho_l\}(\nu_l/M^{0.25})^m]^{k/Y} \times \{g(\rho_l-\rho_v)/\sigma\}^{l/Y}/R^{\{i+k(2m+1)-2l\}/Y} \quad (16)$$

where $Y = 2i+k(m+2)$ and C is made up of various constants, and i, k, l, and m are unknown exponents.

(a) $D_b \lesssim 4$ mm. The variation of bubble frequencies vs bubble diameter shows that the bubbles mainly stay in region II in Fig. 7 due to the small growth rate of bubbles. In this region the drag coefficient in region II in Fig. 7 is given as $C_D = 18.7/Re_d^{2/3}$ by Peebles and Garber [5]. If $m = -2/3$, $\xi\rho_l+\rho_v$ is approximated by $\xi\rho_l$ and the detachment frequency is independent of the Molten number M in correlation (16), then the detachment frequency becomes

$$f = C\{g(\rho_l-\rho_v)/\rho_l\}^{(i+k)/Y}(1/\nu_l)^{2k/3Y} \times \{g(\rho_l-\rho_v)/\sigma\}^{l/Y}/R^{(i-k/3-2l)/Y} \quad (17)$$

where $Y = 2i+4k/3$.

As described in Section 3.2(a), the detachment frequencies of Bobrovich and Mamontova [15] depend on pressure (possibly depending on ν_l and σ) and are almost independent or only weakly dependent on R, and those of the present authors depend weakly on R, and scatter more. The correlations for both measurements can be therefore expressed in the same form with different constants on the basis of correlation (17).

When $f \propto \sigma^{-3/16}$ due to the data by Bobrovich and Mamontova and $(i-k/3-2l)/Y = 1/4$, the following correlation fits the data best at 0.1–5 MPa, measured by Bobrovich and Mamontova and the present authors:

$$f = C\{g(\rho_l-\rho_v)/\rho_l\}^{13/16}(\rho_l^3/\sigma^3\cdot\nu_l^4)^{1/16}R^{1/4} \quad (18)$$

where C is 0.10 for Bobrovich and Mamontova and 0.08–0.13 for the present authors. The predicted results are shown in Figs. 4 and 5.

(b) 4 mm $\lesssim D_b \lesssim$ 15 mm. Peebles and Garber [5] obtained an experimental drag coefficient of $C_D = C(M^{0.25}Re_d)^{9/5}$ for bubbles with constant volume. If, in equation (16), m is assumed to be 9/5 and the sticking force on the wires by surface tension is neglected, so $l = 0$, the bubble detachment frequency is proportional to $R^{-3/4}$, and the constant C is determined to fit the correlation to the data, then

$$f = 0.60\{g(\rho_l-\rho_v)/\rho_l\}^{5/12}(\nu_l/M^{0.25})^{1/6}/R^{3/4}. \quad (19)$$

The dependence of R on detachment frequency is similar to that in the transition region of Ivey. The predictions by correlation (19) are shown in Figs. 4 and 5. The results of the Ivey correlation (5) are also shown in Figs. 4 and 5 by the thick solid lines.

(c) $D_b \gtrsim 15$ mm. The diameter of coalesced bubbles is in region IV in Fig. 7 for most of the growth period before detachment. Here $l = 0$ in equation (16), the bubble detachment frequency is independent of the Molton number M and proportional to $R^{-1/4}$, and m is determined to fit the correlation to the data, so that

$$f = 0.11\{g(\rho_l-\rho_v)/\rho_l\}^{7/12}/(\nu_l^{1/6}R^{1/4}). \quad (20)$$

The measured data of bubble frequencies are weakly dependent on R, maybe due to the upward flow accompanying the bubbles, as in the case of the horizontal upward facing disk.

To obtain the correlation of the macrolayer thickness in correlation (1), the correlation of the bubble frequency must be expressed by the blowing rate of vapor or heat flux. When the growing bubble receives vapor from the length of wire corresponding to the diameter of detached bubbles, the relation between the radius of bubbles and heat flux is obtained by considering mass conservation of vapor as

$$r = (3qdR/2\rho_v H_{fg})^{1/3}t^{1/3} \quad (21)$$

where $G_0 = q/\rho_v H_{fg}$ is used. Putting $r = R$ and $t = 1/f$, correlation (21) becomes

$$R = (3qd/2\rho_v H_{fg})^{1/2}/f^{1/2}. \quad (22)$$

Substituting correlation (22) into the correlations of bubble frequencies (18)–(20) gives the relations between bubble frequency and heat flux or blowing rate of vapor.

For an isolated bubble superheat is introduced into the correlation of bubble frequency, because it is necessary to use the growth relation of primary bubbles,

$$r = CN_{Ja}^{m}(a_1 t)^{1/2} \quad (23)$$

where C is constant and m is from 1/2 to 1, depending on the reference.

5. CONCLUSIONS

The detachment frequency of coalesced bubbles was measured with 2–30 mm diameter disks flush with a horizontal plate and thin 0.1–3 mm diameter wires. The semi-empirical correlations between the frequency f and the blowing rate of vapor (gas) or the radius of detached bubbles were obtained. These correlations are deduced from a dimensional analysis of the force balance equation for bubbles, and unknown constants and exponents in the derived relations are determined to fit the correlations to the measured data. The detachment frequency for horizontal circular disks is weakly dependent on the blowing rate of vapor or gas and is proportional to $D^{-1/3}$. The detachment frequency for horizontal thin wires varies with the diameter of bubbles or the blowing rate, and is classified into three regions with different dependence on the diameter of bubbles.

REFERENCES

1. Y. Katto and S. Yokoya, Principal mechanism of boiling crisis in pool boiling, *Int. J. Heat Mass Transfer* **11,** 993–1002 (1968).
2. Y. Katto and S. Yokoya, Behavior of vapor mass in saturated nucleate and transition pool boiling, *Heat Transfer Jap. Res.* **5,** 45–65 (1976).
3. M. Jakob and W. Linke, *Heat Transfer*, Vol. 1, p. 642. John Wiley, New York (1949).
4. W. Fritz and W. Ende, Verdampfungvorgang nach kinemato-graphischen Aufnahmen an Dampfblasen, *Phys. Z.* **35,** 391–401 (1936).
5. F. N. Peebles and H. J. Garber, Studies on the motion of gas bubbles in liquids, *Chem. Engng Prog.* **49,** 88–97 (1953).
6. N. Zuber, Nucleate boiling—the region of isolated bubbles and the similarity with natural convection, *Int. J. Heat Mass Transfer* **6,** 53–78 (1963).
7. K. Yamagata, F. Hirano, K. Nishikawa and H. Matsuoka, Nucleate boiling of water on the horizontal heating surface, *Trans. JSME* **18–67,** 53–56 (1952) (in Japanese).
8. T. H. K. Frederking and D. J. Daniels, The relation between bubble diameter and frequency of removal from a sphere during film boiling, *ASME J. Heat Transfer* **88,** 87–93 (1966).
9. H. J. Ivey, Relationships between bubble frequency, departure diameter and rise velocity in nucleate boiling, *Int. J. Heat Mass Transfer* **10,** 1023–1040 (1967).
10. R. Cole, A photographic study of pool boiling in the region of critical heat flux, *A.I.Ch.E. Jl* **6,** 533–538 (1960).
11. S. Maeda, Review of bubble formation and its movement, *Kagaku Kogaku (Chem. Engng Jap.)* **31,** 438–443 (1967) (in Japanese).
12. Y. Iida and K. Kobayasi, An investigation on the mechanism of pool boiling phenomena by a probe method, *Proceedings of the 4th International Heat Transfer Conference*, Vol. 5, pp. 1–11 (1970).
13. H. Honda and K. Nishikawa, Study of boiling curve around transition boiling, *Trans. JSME* **34**(257), 177–184 (1972) (in Japanese).
14. J. F. Davidson and O. G. Schüler, Bubble formation at an orifice in an iviscid liquid, *Trans. Instn Chem. Engrs* **38,** 335–345 (1960).
15. G. I. Bobrovich and N. N. Mamontova, A study of the mechanism of nucleate boiling at high heat fluxes, *Int. J. Heat Mass Transfer* **8,** 1421–1424 (1965).
16. A. S. Perkins and J. W. Westwater, Measurements of bubbles formed in boiling methanol, *A.I.Ch.E. Jl* **2,** 471–476 (1956).
17. K. Yamagata, F. Hirano, K. Nishikawa and H. Matsuoka, Nucleate boiling of water on the horizontal heating surface, *Mem. Fac. Engng Kyusyu Univ.* **15,** 97–163 (1955).
18. N. Zuber, Hydrodynamic aspects of boiling heat transfer, A.E.C.U. Report No. 4439 (1959).